

NACA RM E57HO7a

UNCLASSIFIED

U-2

# NACA

## RESEARCH MEMORANDUM

PERFORMANCE OF EXTERNAL-INTERNAL COMPRESSION  
INLET WITH ABRUPT INTERNAL TURNING AT  
MACH NUMBERS 3.0 TO 2.0

By Leonard J. Obery and Leonard E. Stitt

Lewis Flight Propulsion Laboratory  
Cleveland, Ohio

CLASSIFICATION CHANGED

UNCLASSIFIED

*Effect of  
1-12-64  
authenticity of J.A. # 39*

**LIBRARY COPY**

OCT 22 1957

LANGLEY AERONAUTICAL LABORATORY  
LIBRARY, NACA  
LANGLEY FIELD STATION, VIRGINIA

CLASSIFIED DOCUMENT

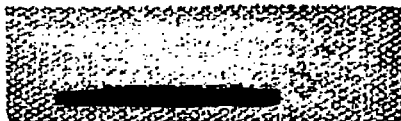
This material contains information affecting the National Defense of the United States within the meaning of the espionage laws, Title 18, U.S.C., Secs. 793 and 794, the transmission or revelation of which in any manner to an unauthorized person is prohibited by law.

### NATIONAL ADVISORY COMMITTEE FOR AERONAUTICS

WASHINGTON

October 21, 1957





## NATIONAL ADVISORY COMMITTEE FOR AERONAUTICS

RESEARCH MEMORANDUMPERFORMANCE OF EXTERNAL-INTERNAL COMPRESSION INLET WITH  
ABRUPT INTERNAL TURNING AT MACH NUMBERS 3.0 TO 2.0

By Leonard J. Obery and Leonard E. Stitt

## SUMMARY

4600

CL-1

An inlet with combined external and internal supersonic compression, formed by spike and cowl oblique shocks, and an over-all length of  $2\frac{1}{2}$  inlet diameters was investigated at Mach numbers from 3.0 to 2.0 over a range of angles of attack. At the design Mach number of 3.0 the low angle cowl, which turned the flow supersonically, generated two internal shocks and focused them on the centerbody surface. These compression waves, with their high pressure gradient, were cancelled by abrupt centerbody turning. This investigation showed that with proper boundary-layer control on the centerbody this method of internal compression did not adversely affect the high performance of the inlet. For example, a pressure recovery of 0.78 was obtained at Mach number 3.0 with a cowl drag coefficient of 0.01. A high distortion (23 percent) resulted from the short length, high diffusion rate, and high discharge Mach number of this particular design. Supersonic spillage by the external oblique shock at lower Mach numbers gave relatively low drag increases. At Mach number 2.0, 50 percent of the flow was spilled with an over-all drag of only 0.125. The inlet was sensitive to type of centerbody bleed. A ram-scoop configuration forced centerbody boundary-layer separation; the added turning prevented design-point operation of the inlet, and hence lower recoveries were obtained than with the flush-slot configuration.

## INTRODUCTION

One method of obtaining a low cowl projected area, with its attendant reduction in cowl drag, was demonstrated in reference 1. The high-angle flow from an all-external-compression inlet was turned back to an axial direction through the use of rapid turns on the cowl and centerbody surfaces.



It is possible to reduce the cowl area further by turning the internal flow supersonically, utilizing the relatively straight cowl as a reflecting plane. The present investigation was therefore conducted on an external-internal-compression inlet to determine the feasibility of (1) turning the internal flow supersonically and thereby reducing the cowl drag, and (2) imposing a high pressure gradient on the centerbody surface without adversely affecting the internal performance. The overall length of the inlet, with an equivalent  $12^\circ$  conical area expansion subsonic diffuser, was  $2\frac{1}{2}$  inlet diameters.

## SYMBOLS

A	flow area
$A_{\max}$	maximum frontal area, 283.5 sq in.
$A_3$	diffuser-exit area, 119.94 sq in.
$C_D$	drag coefficient, $D/q_0 A_{\max}$
D	drag
l	distance from cowl lip to diffuser-exit station
M	Mach number
m	mass flow
P	total pressure
p	static pressure
q	dynamic pressure, $\frac{\gamma p M^2}{2}$
w	weight flow
$\frac{w\sqrt{\theta}}{\delta A}$	corrected weight flow per unit area
x	lineal distance
$\alpha$	angle of attack
$\gamma$	ratio of specific heats for air, 1.4
$\delta$	ratio of total pressure to NACA standard sea-level pressure

$\theta$  ratio of total temperature to NACA standard sea-level temperature

$\theta_7$  angle between cone tip and cowl lip and axis of model

Subscripts:

a additive

av average

c cowl

max maximum

min minimum

x condition at x-distance

0 free-stream

3 diffuser-exit station

## APPARATUS AND PROCEDURE

### Model

The centerbody and cowl of the inlet were designed and adapted to the existing afterbody of the 19-inch axisymmetric inlet model reported in reference 1. The model was sting-mounted in the tunnel, and angle of attack was varied to  $15^\circ$  by means of the support strut. Mass flow through the model was regulated by the remotely actuated control plug.

### Design Details

At the design Mach number of 3.0, the oblique shock from the  $20^\circ$ -half-angle cone intercepted the cowl lip. A photograph of the inlet with the spike in its design position is shown in figure 1(a). The internal cowl angles were designed to turn the supersonic flow back toward the model axis in two steps of  $12^\circ$  each. The two resulting oblique shocks from the cowl impinged at a common axial station on the centerbody as shown in figure 2. The centerbody was turned abruptly at this point to align the surface with the resulting flow. An internal bleed, either flush slot or ram scoop, was located around the perimeter of the centerbody immediately forward of this station to remove the spike boundary-layer air prior to the high pressure rise through the internal oblique shocks. A photograph of the flush-slot inlet is presented in figure 1(b).

The bleed air was ducted from the centerbody and returned to free-stream through the hollow support struts, as shown in figure 2. Subsonic diffusion was completed at model station 26.5 (fig. 2) with a resulting over-all length, from cone tip to diffuser exit, of only  $2\frac{1}{2}$  inlet diameters.

The external cowl-lip angle was held constant at  $7\frac{1}{4}^\circ$  back to the maximum body diameter, the resulting projected area of the cowl being about 9 percent of the inlet frontal area. Pertinent areas were as follows:

Projected cowl-lip area, 257.2 sq in.  
Maximum frontal area, 283.5 sq in.  
Diffuser-exit area, 119.94 sq in.

The inlet was matched to a hypothetical engine at off-design speeds by translating the spike forward, which reduced the capture mass flow and increased the throat area, as shown in figure 2. Internal flow areas for some typical spike extensions are indicated in figure 3.

#### Calculations and Instrumentation

Inlet mass flow was computed from measured static pressure at the diffuser-exit station of the original model (station 66, fig. 2) and a choked plug. A calibration factor, based on the results of reference 1, was applied to the computed mass flows. The mass flow was referenced to the maximum capture mass flow defined by the projected area of the inlet lip at zero angle of attack.

The diffuser-exit total-pressure recovery, distortion, and contours were based on rake measurements at station 26.5. The distortion parameter presented is defined as the difference between the maximum and minimum total pressure indicated by individual tubes in the exit rakes, divided by the rake average pressure.

Additional total-pressure rakes were located on the centerbody ahead of and behind the bleed slot, on the cowl at the location of the second internal oblique shock, and across the duct annulus at station 2.

Static-pressure taps were distributed axially on the centerbody and cowl. External cowl static pressures were used to compute the cowl drag coefficient at zero angle of attack.

The investigation was conducted in the Lewis 10- by 10-foot supersonic wind tunnel at Mach numbers from 3.0 to 2.0 and a Reynolds number of  $2.5 \times 10^6$  per foot

## RESULTS AND DISCUSSION

The internal performance of the flush-slot configuration, for a fixed spike projection, is shown in figure 4 at Mach number 3.0 and zero angle of attack. The curve is typical of the operation of an internal-compression inlet. In the supercritical region the mass flow was constant and the recovery increased until the normal shock was regurgitated, resulting in the discontinuity of the mass-flow - pressure-recovery curve, as shown. The performance fell off along a line of constant corrected weight flow to a recovery level equal to a single  $20^\circ$  conical inlet. (For an all-internal-compression inlet normal-shock recovery would be expected if the shock was regurgitated, and consequently an even lower mass-flow ratio would result.)

Figure 5 presents a trace of the variation in static and total pressure at the diffuser-exit station as the inlet terminal shock was expelled at Mach 3.0. When the shock was regurgitated the inlet buzzed at about 10 cycles per second with a total-pressure amplitude of about 11 percent of free-stream total pressure.

The peak-recovery points at various spike projections are presented in figure 6 as the over-all performance of the flush-slot configuration over a range of Mach numbers and angles of attack. The data represent a flow condition that could be maintained stably for a long period of time. Pressure recoveries about 1 percent higher than those shown could be attained in most cases; however, shock-swallowed flow could not be maintained indefinitely at these recoveries. The highest values of spike-position parameter presented generally represent the most rearward retraction of the spike, concurrent with shock-swallowed flow. When the spike could be retracted past the peak-recovery position, as at  $M_0 = 2.8$ , the decrease in maximum recovery was very rapid.

The distortions measured at the diffuser exit (station 26.5) were quite high, from about 30 percent of diffuser-exit pressure at the higher Mach numbers to about 10 percent at lower Mach numbers. The high distortion levels of this inlet are probably due to its short length, high diffusion rate, and high discharge Mach number, all of which have been shown to affect distortion adversely (refs. 2 to 4). A comparison of the distortion level between the diffuser exit of the present investigation (station 3) and the diffuser exit of the previous model of reference 1 (station 4) indicated that the added mixing length reduced the distortions to about 3 to 6 percent at Mach 3.0. Only a slight amount of additional diffusion occurred between these two stations.

The cowl pressure-drag coefficient varied from about 0.01 at Mach 3.0 to about 0.005 at Mach 2.0, based on frontal area. Calculations were made, based on reference 5, of the supersonic additive drag developed by

the 20° cone at lower than shock-on-lip spike-position-parameter values. These calculated additive drags were added to the measured pressure drags, and the total is presented as the dashed lines in figure 6. The total drag coefficient at the highest spike-position parameter varied from 0.01 at Mach 3.0 to 0.125 at Mach 2.0. The friction drag was not measured on this model; however, based on the drag breakdown presented in reference 1, the friction drag coefficient on the portion of the model to the diffuser-exit station might be on the order of 0.004.

The critical mass-flow characteristics of the inlet are shown in figure 7. At Mach 3.0 for shock-on-lip operation about 2 percent of the capture mass flow was removed through the bleed system. Presumably, about this amount of flow was bled from the inlet at other conditions. The limited amount of angle-of-attack data taken during the test represents the maximum-pressure-recovery points as determined by visual observations and control-room calculations. At 15° angle of attack, for example, it was possible to capture somewhat more mass flow than the value shown; however, the pressure recovery dropped rapidly from the point presented. Generally, the inlet appeared to regurgitate the shock whenever the oblique shock from the cone tip first intersected the bottom of the cowl lip. At Mach 2.0 and 0° angle of attack, it was not possible to capture more than about 50 percent mass-flow ratio before shock regurgitation. The angle-of-attack effects, however, were considerably reduced from those obtained at the higher Mach numbers. Corrected-weight-flow lines are plotted on the figure for each Mach number. The corrected weight flow furnished by the inlet increased from 31 to 35 as the Mach number decreased from 3.0 to 2.5 and then remained essentially constant to Mach 2.0. At Mach 2.4 the second oblique shock off the cowl lip approached detachment, and apparently the detached-shock condition regulated the corrected weight flow for the Mach number range below 2.4.

The angle-of-attack performance of the inlet was comparable to that of an all-external-compression inlet (inlet I with bleed, ref. 6), as shown in figure 8. The external-internal-compression inlet, however, spilled considerably more mass flow at the lower Mach numbers.

Very high distortions were measured at angle of attack. As with other inlet types, the high-energy air tended to follow a straight line and, as shown in figure 9, the high-energy cores shifted to the top of the diffuser annulus at the higher angles of attack. Individual tubes, not shown on the contour map, showed a distortion of 109 percent at 15° angle of attack. The strut shown in the passage was a structural part of the previous model rather than an integral part of the present design. In an actual installation it would not be present, and the contours would become annular instead of having the lobe shapes presented.

Detailed rake measurements are presented in figure 10 to demonstrate that a high pressure gradient can be imposed on the centerbody surface.

4600

Calculations indicated the coalescence of the two cowl waves should produce a static pressure ratio of about 3.7 at the design Mach number of 3.0. Pitot rakes were located on the cowl and centerbody surfaces as shown in figure 10, and a row of static orifices measured the pressures on the centerbody. At Mach 3.0 the cowl and spike rakes indicated the shocks from the cowl lip were about the predicted strength and were located at the proper position; that is, they impinged on the centerbody at the shoulder. The station 1 rake shows a fairly thin boundary layer and no separated region, because all the tubes out of the boundary layer are at the theoretical pressure recovery. At Mach 2.5 (about the limit of attachment for the second shock off the cowl) the spike rake shows a thin boundary layer and again no separated region. The cowl rake, however, shows bridging or possible flow separation across the cowl break. The station 1 rake again shows no separation from the centerbody but does show, by the increased recovery of the outer tubes, an increased compression from the cowl. At Mach 2.0 the second shock off the cowl should be detached and, from the recovery of the cowl rake, it appears that the cowl lip does not even form an oblique shock but rather a normal shock. This deduction was also substantiated by cowl static pressures (not presented), which indicated about  $20^\circ$ -cone plus normal-shock static pressures existing from the cowl lip rearward into the inlet. The spike rake shows a separated boundary layer with the attendant oblique shock passing between the outer two tubes. The last tube (0.75 in. from surface) reads the pressure recovery of a Pitot tube behind only the  $20^\circ$ -half-angle-cone shock. The recovery level of the center two tubes, as well as the static-pressure measurements in this location on the spike, corresponds to a separation region of about a  $12^\circ$  angle.

A rake was also located at station 2, about one-fourth of the distance between stations 1 and 3, where about one-third of the subsonic diffusion had taken place at the Mach 3.0 design spike position. Integration of the rakes at stations 1 and 2 shows that approximately all the subsonic-diffuser loss had occurred between these two stations and that the remaining diffusion was almost isentropic. Because this was the high-loss region, it is hypothesized that boundary-layer control, perhaps in the form of area suction on both the centerbody and the cowl, would provide increased recovery by removing the low-energy regions shown by the station 2 rake.

The inlet was quite sensitive to the type of spike boundary-layer bleed. A ram scoop, designed to remove about the same amount of flow as the flush slot, was located at the centerbody break. With the ram-scoop configuration the spike could not be retracted into the design position at Mach number 3.0, and the peak recovery was considerably lower than with the flush-slot configuration (fig. 11). At Mach 2.0 about the same recovery level was reached but with a considerably extended spike position and, of course, at a lower mass-flow ratio. The pressure distribution on the spike shows that the ram scoop forced a boundary-layer separation, and

this added turning would not allow the spike to be retracted to the design positions. The concept that a ram scoop can cause a boundary-layer separation by its own presence, without the aid of a strong shock pressure rise, is also presented in reference 6. It appears from the data that, even though the separated region was bled from the inlet by the ram scoop, the extra turning prevented design-point operation of the inlet. This implies that a ram-scoop bleed might not be suitable for internal-compression inlets.

A larger flush-slot configuration was also investigated. The throat area of the bleed was about double that for the previous configuration. The peak recovery attained with this configuration was about 1 to 2 percent lower than the data presented earlier herein, although, within the accuracy of the measurements, about the same amount of mass flow was bled from the inlet.

4600

#### SUMMARY OF RESULTS

An inlet with a 20°-half-angle external conical compression surface, two internal-compression surfaces formed by the cowl, and an over-all length of  $2\frac{1}{2}$  inlet diameters was investigated at Mach numbers from 2.0 to the design value of 3.0. Turning the internal flow supersonically with a low-angle cowl resulted in a high pressure gradient on the centerbody surface. The following results were obtained:

1. The inlet performance indicated that the flow could successfully be turned internally and supersonically by the oblique shocks off the cowl. Detailed rake measurements showed the practicality of imposing a high pressure gradient on the centerbody surface by using a proper bleed system and by the cancellation of the waves by a sharp turn on the centerbody.
2. At Mach 3.0 the inlet gave high pressure recovery (0.78) with a very low drag coefficient (0.01). The high distortions (23 percent) resulted from the short length, high diffusion rate, and high discharge Mach number of this particular inlet design. The internal supersonic flow behaved about as predicted.
3. At lower Mach numbers, the cowl pressure drag decreased. Supersonic spillage from the conical oblique shock gave relatively low drag increases; at Mach 2.0, 50 percent of the flow was spilled with a total drag coefficient of only 0.125.
4. The inlet performance was sensitive to the type of centerbody bleed. A ram-scoop configuration forced a spike boundary-layer separation

and, because of the added turning, limited the spike retraction to values considerably less than design, thus yielding lower total-pressure recoveries and higher mass-flow spillages at all Mach numbers.

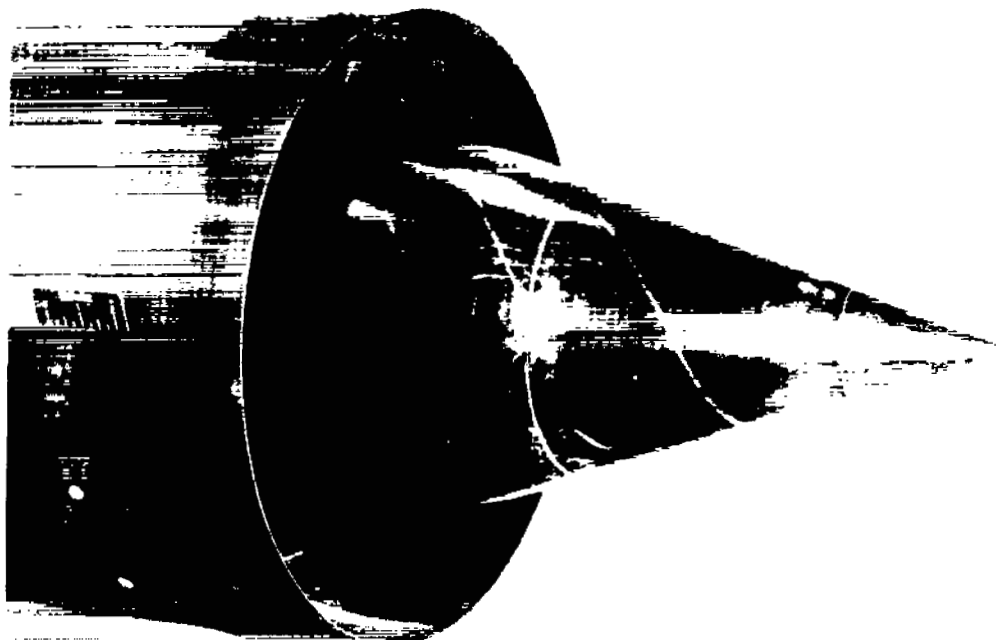
Lewis Flight Propulsion Laboratory  
National Advisory Committee for Aeronautics  
Cleveland, Ohio, August 16, 1957

#### REFERENCES

1. Connors, James F., Wise, George A., and Lovell, J. Calvin: Investigation of Translating-Double-Cone Axisymmetric Inlets with Cowl Projected Areas of 40 and 20 Percent of Maximum at Mach Numbers from 3.0 to 2.0. NACA RM E57C06, 1957.
2. Piercy, Thomas G.: Factors Affecting Flow Distortions Produced by Supersonic Inlets. NACA RM E55L19, 1956.
3. Sterbenz, William H.: Factors Controlling Air-Inlet Flow Distortions. NACA RM E56A30, 1956.
4. Squire, H. B.: Experiments on Conical Diffusers. Aeronautical Research Council Reports and Memoranda No. 2751, November 1950.
5. Sibulkin, Merwin: Theoretical and Experimental Investigation of Additive Drag. NACA Rep. 1187, 1954. (Supersedes NACA RM E51B13.)
6. Connors, James F., Lovell, J. Calvin, and Wise, George A.: Effects of Internal-Area Distribution, Spike Translation, and Throat Boundary-Layer Control on Performance of a Double-Cone Axisymmetric Inlet at Mach Numbers from 3.0 to 2.0. NACA RM E57F03, 1957.

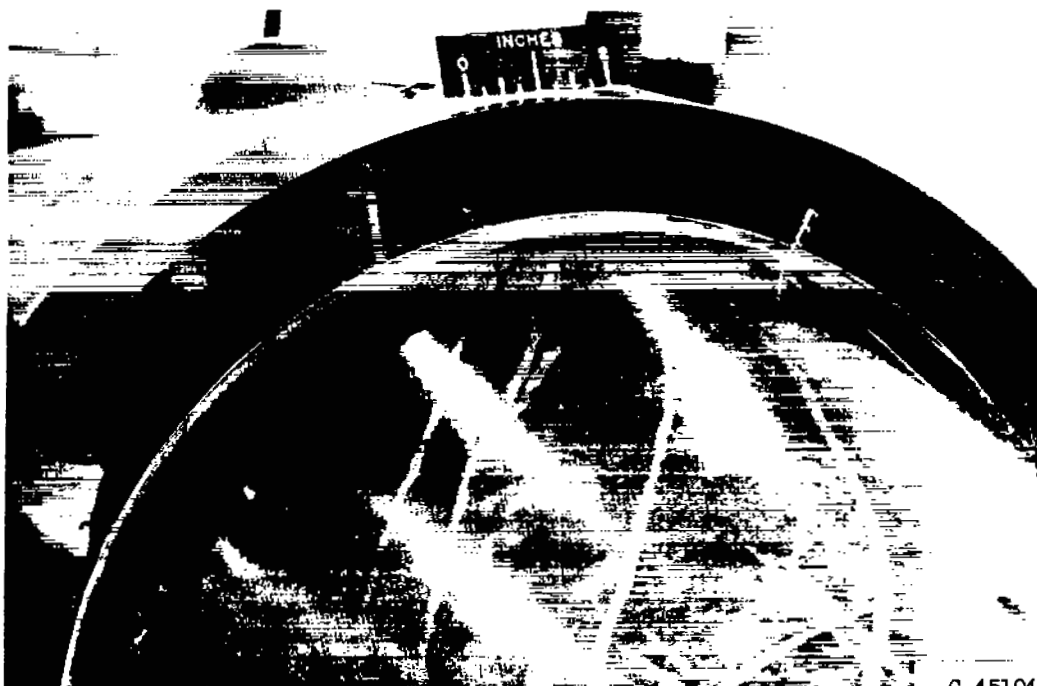
4600

.CL-2



C-45103

(a) Spike retracted to design position.



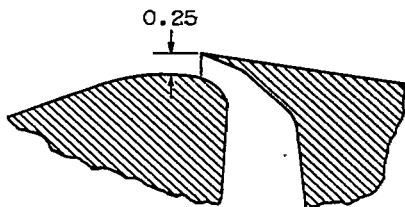
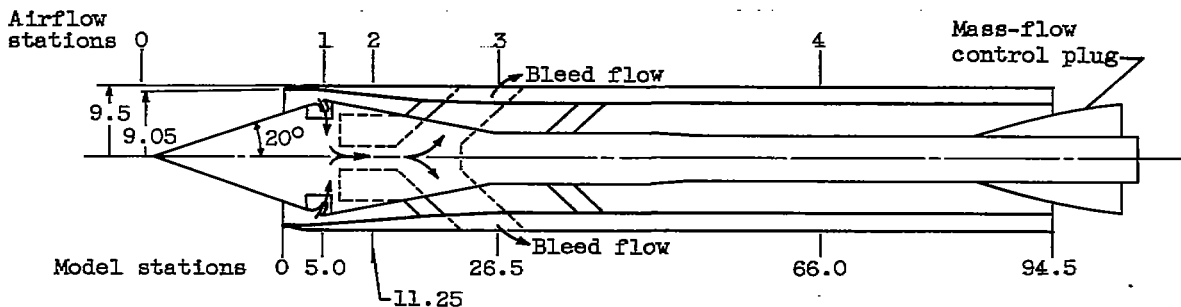
C-45104

(b) Boundary-layer bleed, spike extended.

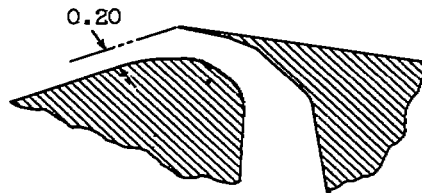
Figure 1. - Photographs of model.

4600

CL-2 back

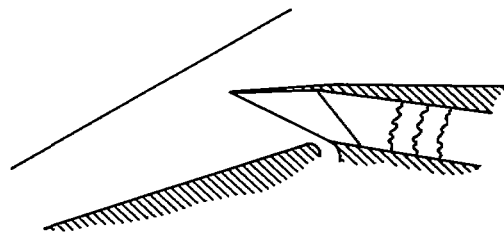
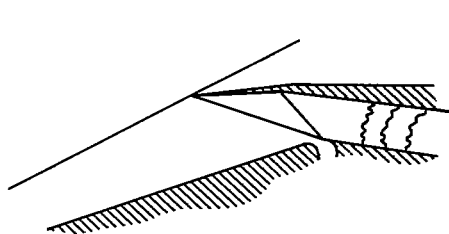


Flush-slot bleed



Ram-scoop bleed

Details of internal shoulder bleed



Theoretical shock locations

CD-5820

Figure 2. - Model details. (All dimensions in inches.)

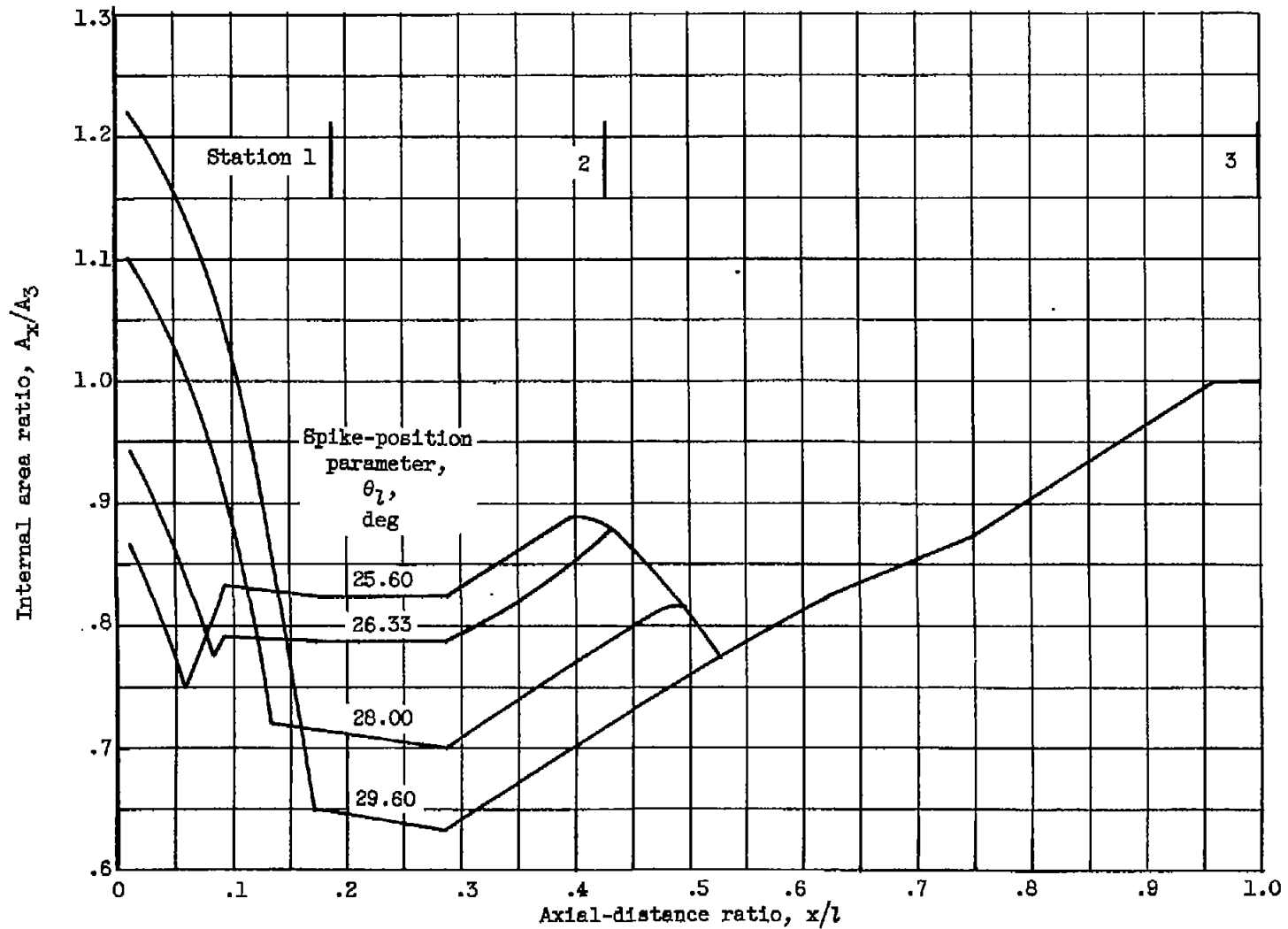


Figure 3. - Internal area variation. (Length of diffuser,  $l$ , 26.6 in.; diffuser-exit area,  $A_3$ , 119.94 sq in.)

4600

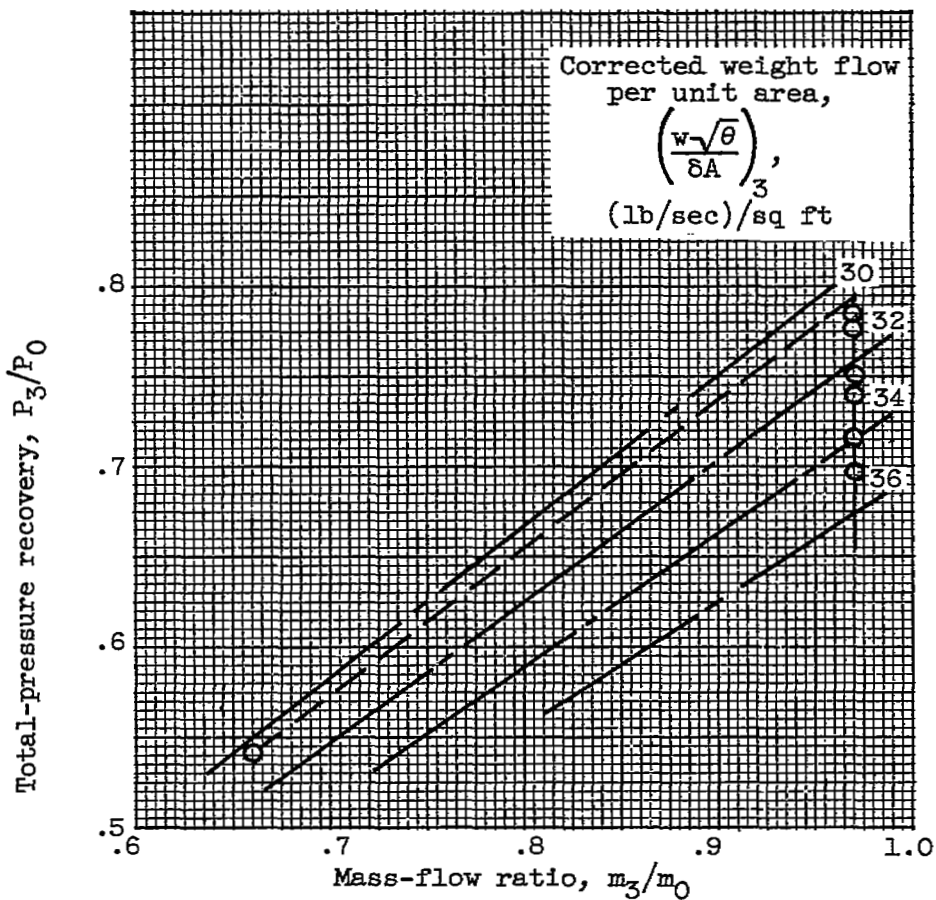


Figure 4. - Internal performance of flush-slot configuration at Mach 3.0 with spike position parameter of  $29.85^\circ$ .

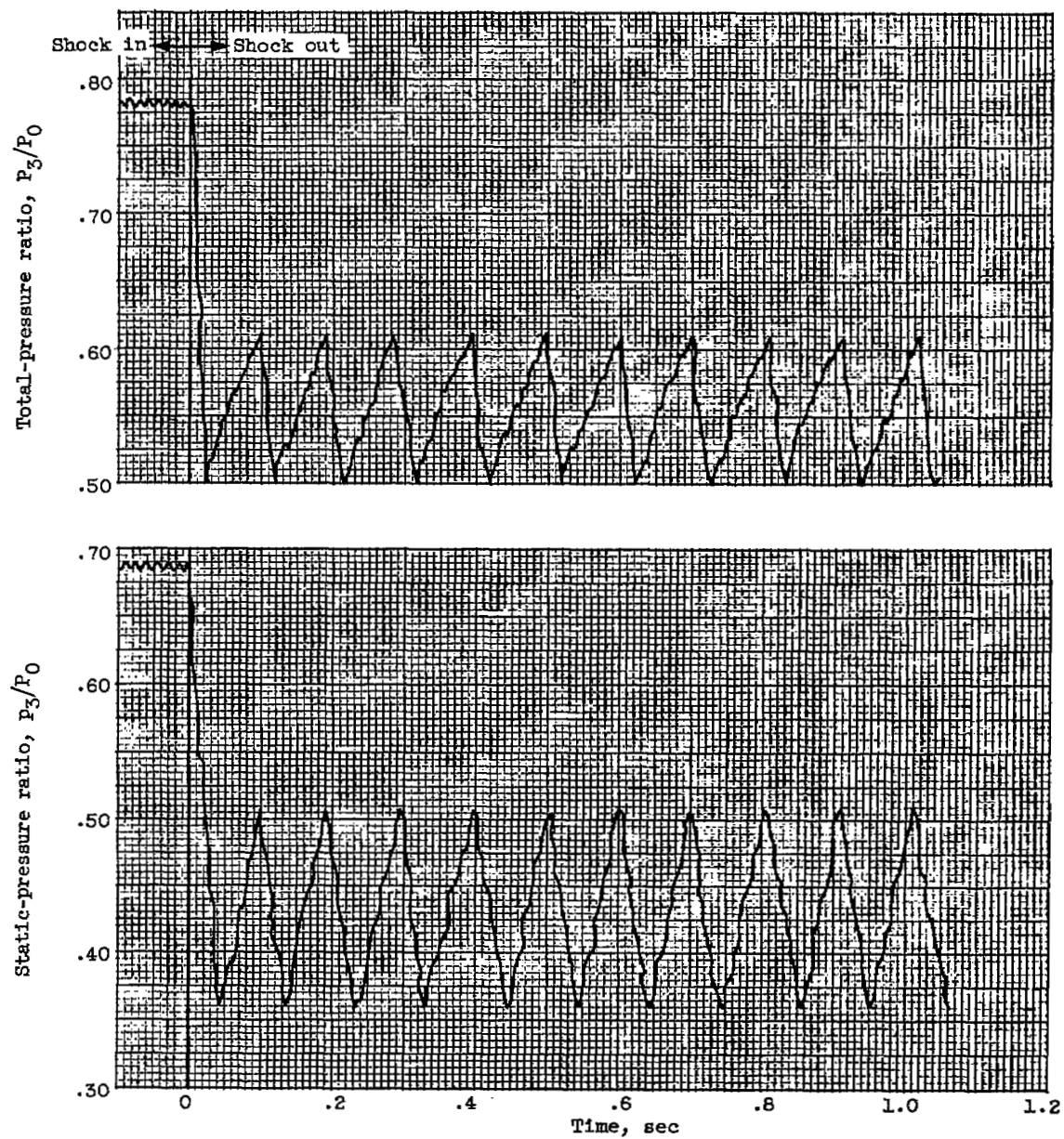


Figure 5. - Transient pressure traces as normal shock is expelled at Mach 3.0. Spike-position parameter,  $29.85^\circ$ ; angle of attack,  $0^\circ$ .

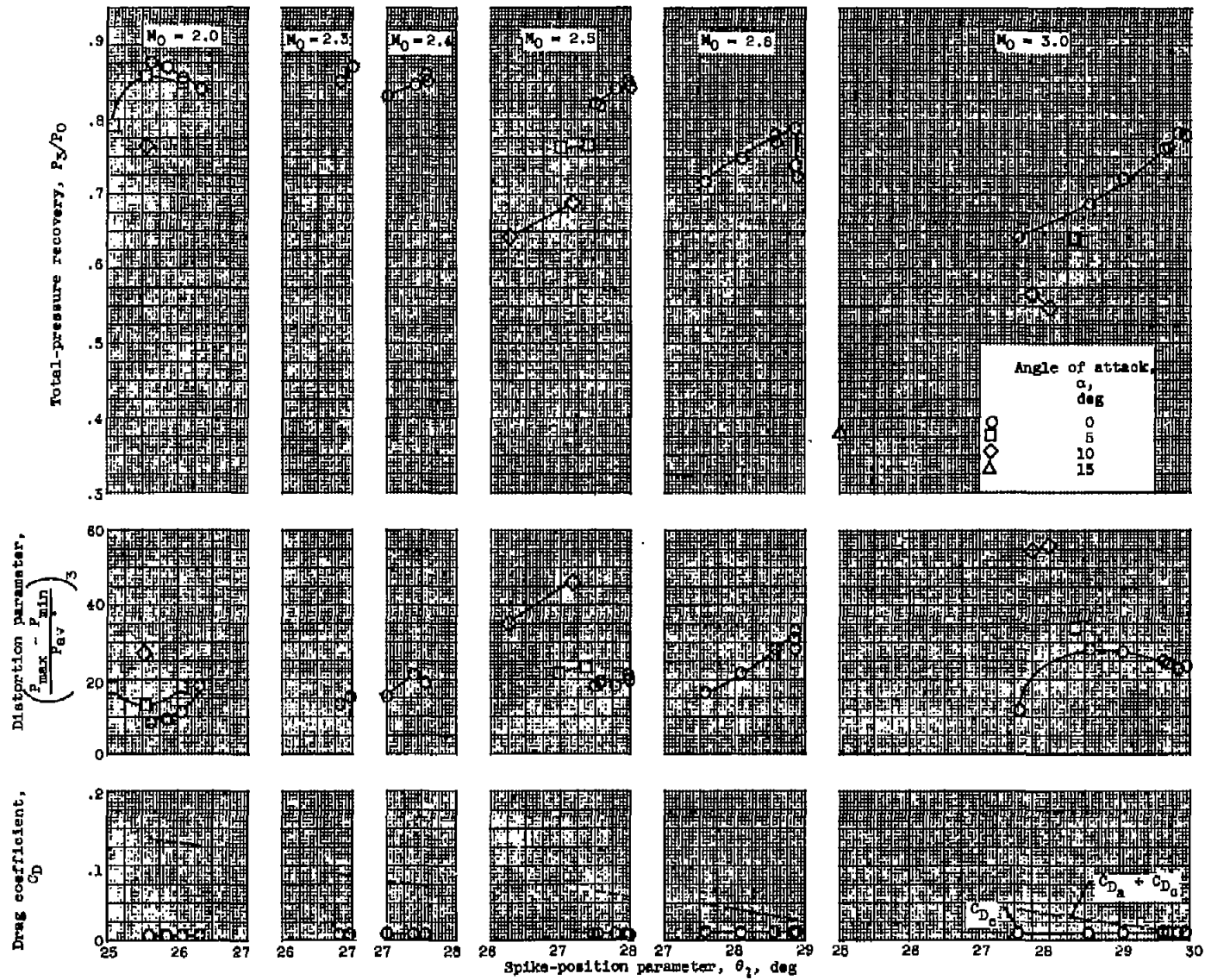


Figure 6. - Over-all performance of flush-slot configuration.

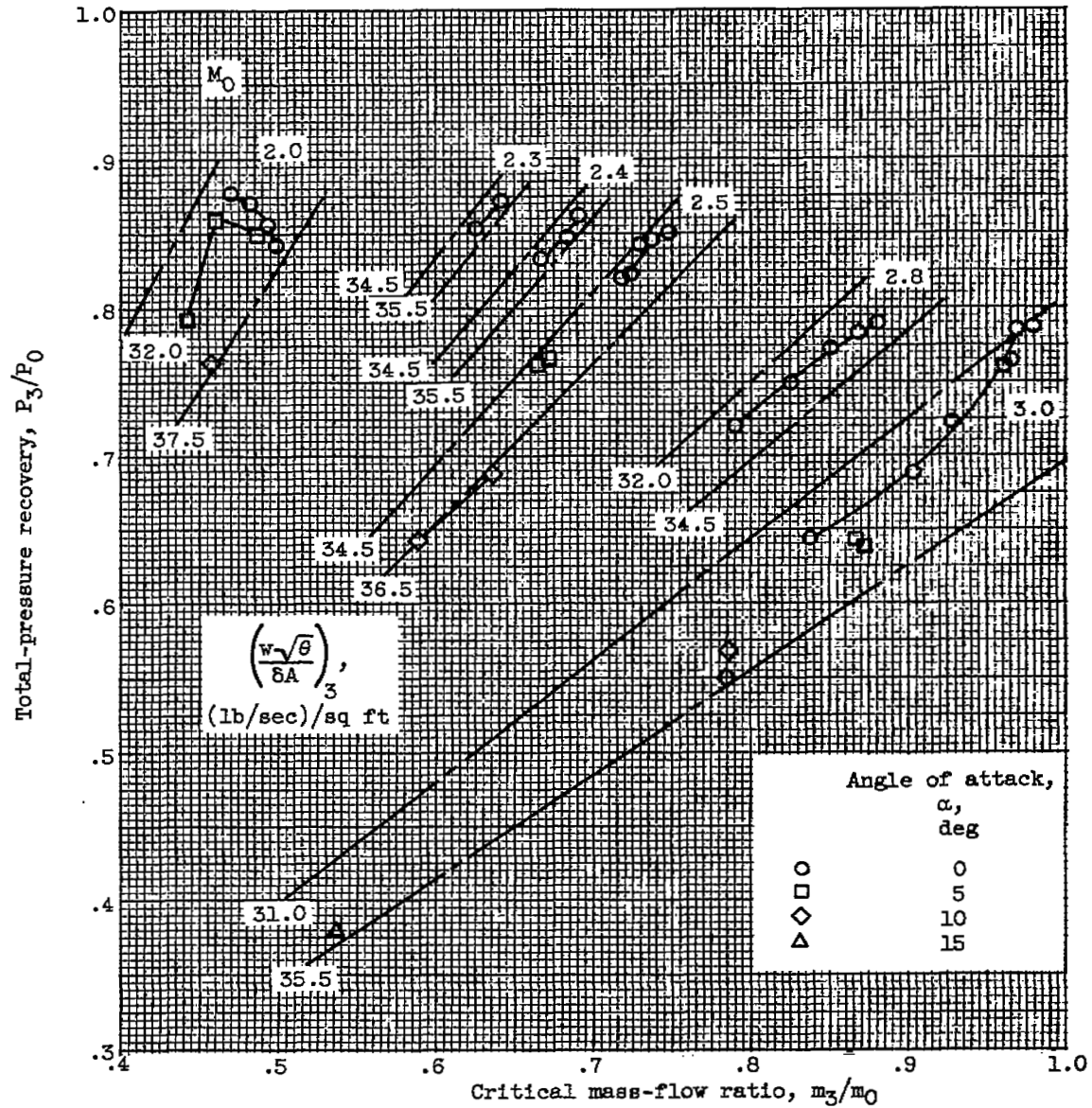


Figure 7. - Internal performance of flush-slot configuration. (Points are for various spike-position parameters.)

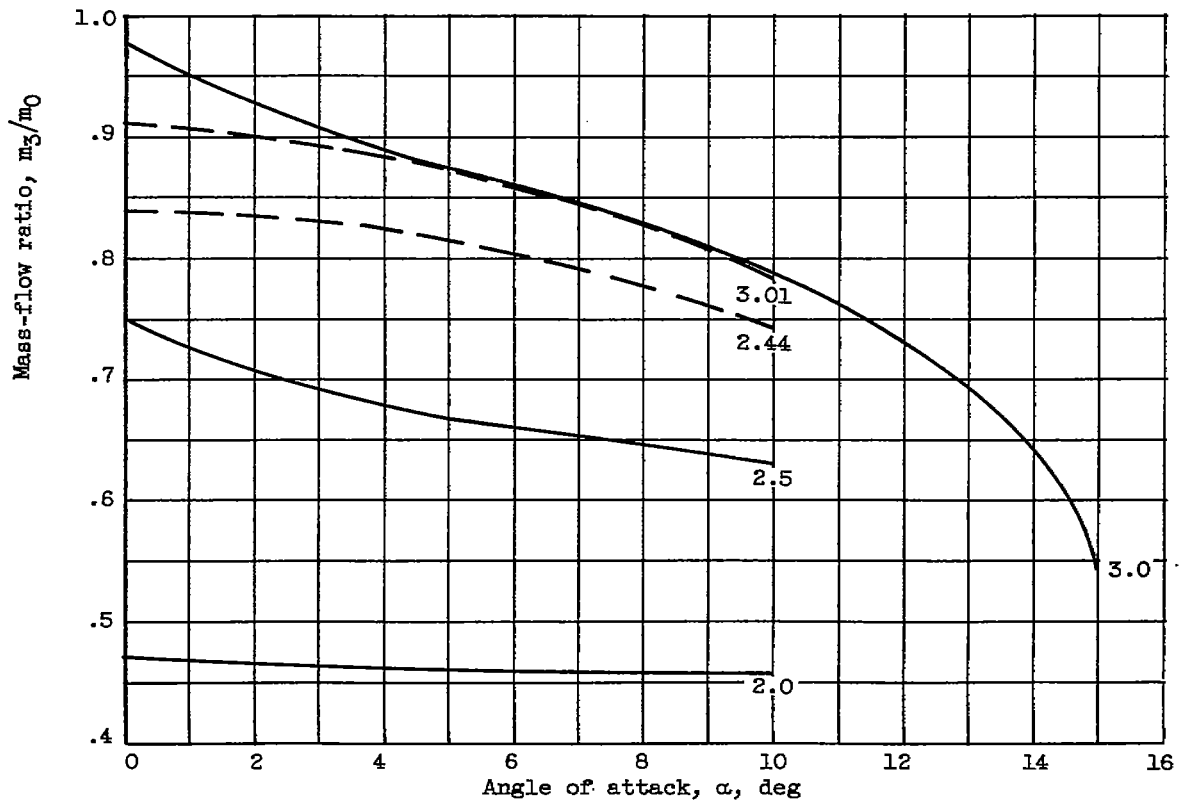
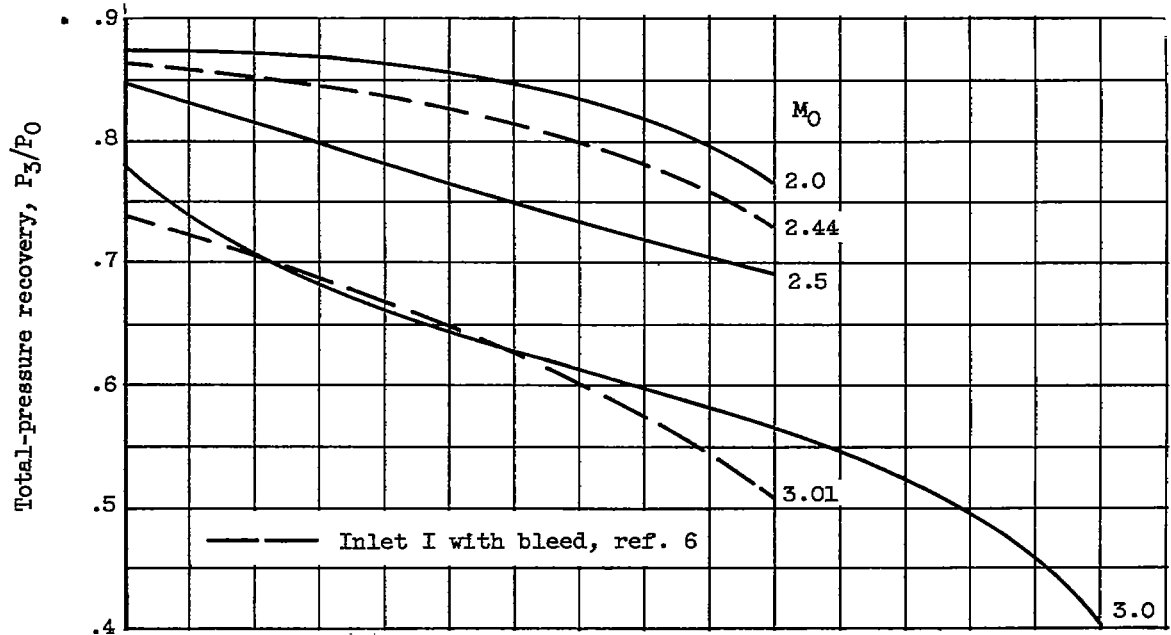


Figure 8. - Angle-of-attack characteristics of flush-slot inlet.

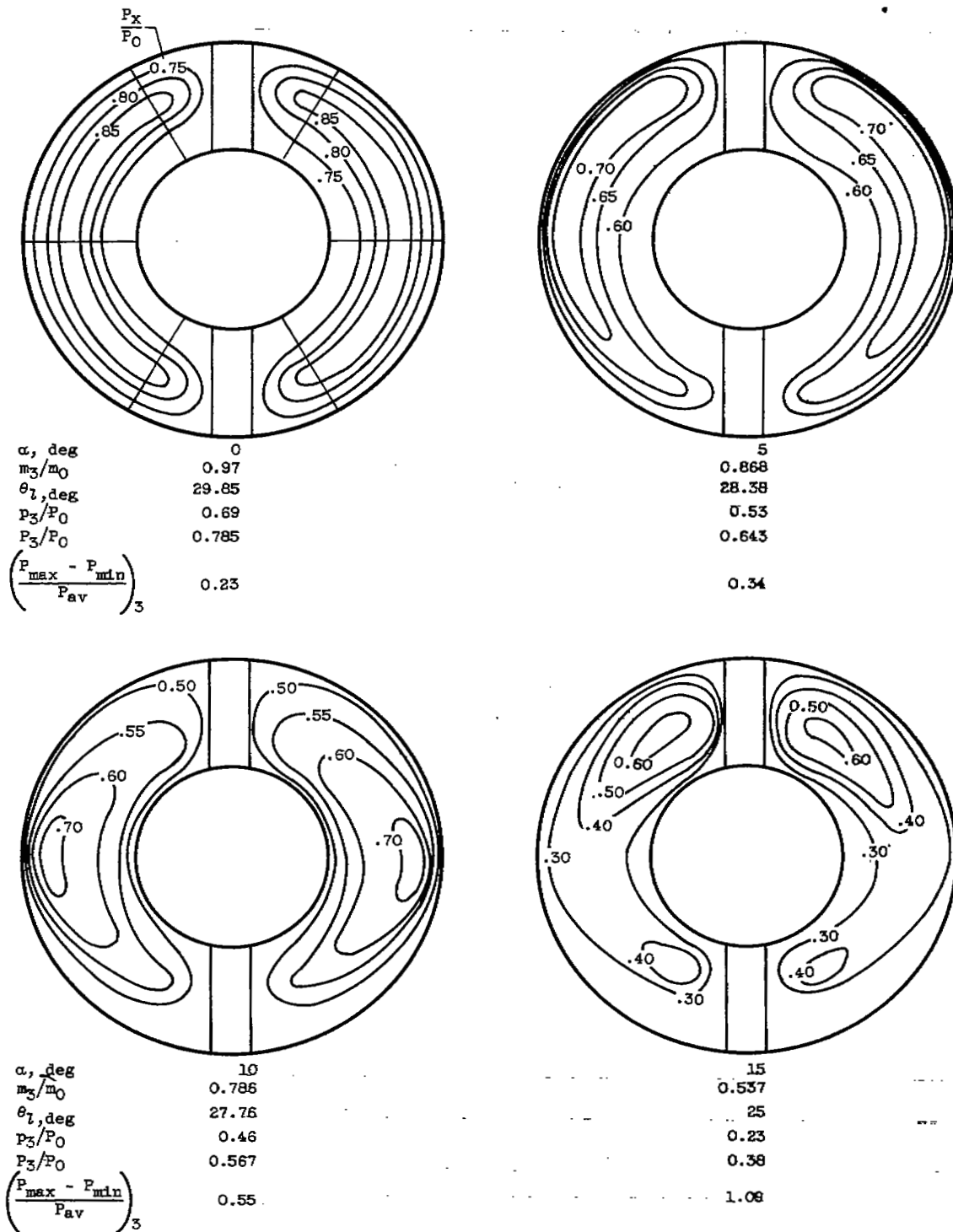


Figure 9. - Total-pressure contours for flush-slot configuration at Mach number 3.0.

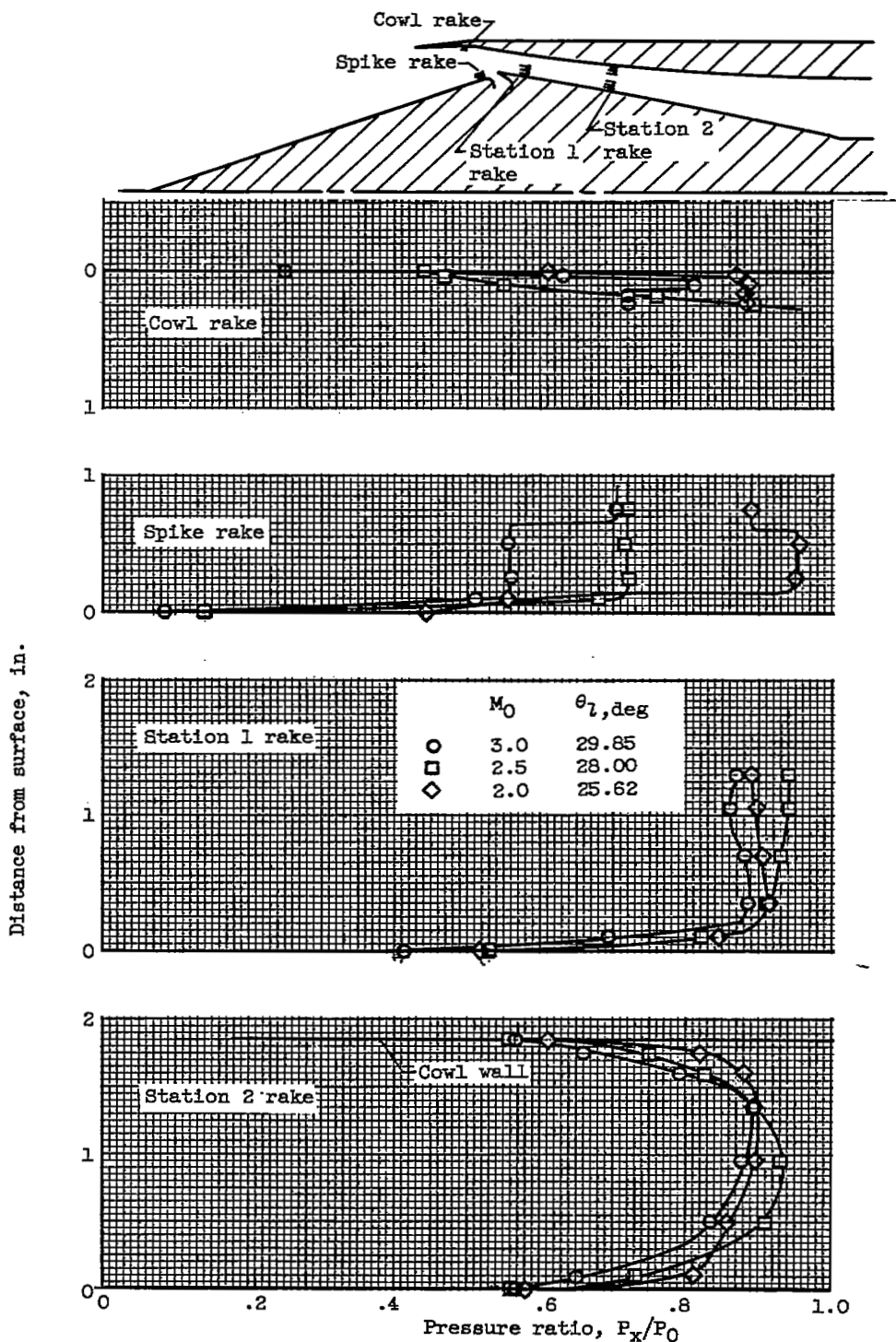


Figure 10. - Pitot pressure measurements at several locations in duct for flush-slot configuration.

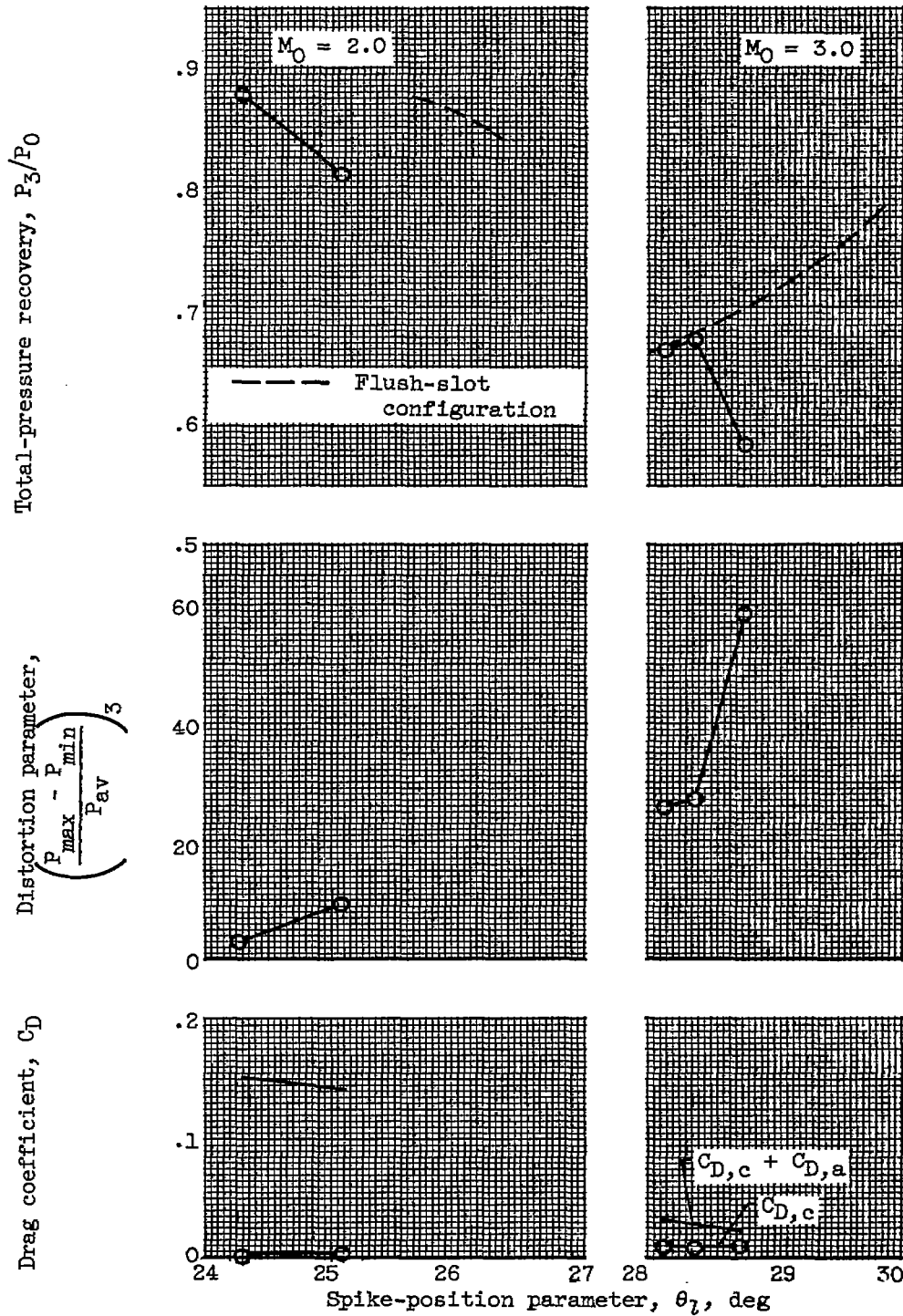


Figure 11. - Over-all performance of ram-scoop configuration.

NOTES: (1) Reynolds number is based on the diameter of a circle with the same area as that of the capture area of the inlet.

(2) The symbol \* denotes the occurrence of buzz.

Report and facility	Description			Test parameters				Test data			Performance		Remarks	
	Configuration	Number of oblique shocks	Type of boundary-layer control	Free-stream Mach number	Reynolds number $\times 10^{-6}$	Angle of attack, deg	Angle of yaw, deg	Drag	Inlet-flow profile	Discharge-flow profile	Flow picture	Maximum total-pressure recovery		Mass-flow ratio
CONFID. RM 857807A Lewis 10- by 10-foot supersonic wind tunnel		3	Flush slot and ram scoop at center-body shoulder	2.0 to 3.0	3.78	0°-15°	0	✓	✓	✓		At $M_0 = 3.0$ , $P_3/P_0 = 0.785$ ; at $M_0 = 2.0$ , $P_3/P_0 = 0.875$	At $M_0 = 3.0$ , $m_3/m_0 = 0.98$ ; at $M_0 = 2.0$ , $m_3/m_0 = 0.50$	External-internal supersonic compression, short-length diffuser. Low cowl projected area resulted from internal supersonic turning of flow.
CONFID. RM 857807A Lewis 10- by 10-foot supersonic wind tunnel		3	Flush slot and ram scoop at center-body shoulder	2.0 to 3.0	3.78	0°-15°	0	✓	✓	✓		At $M_0 = 3.0$ , $P_3/P_0 = 0.785$ ; at $M_0 = 2.0$ , $P_3/P_0 = 0.875$	At $M_0 = 3.0$ , $m_3/m_0 = 0.98$ ; at $M_0 = 2.0$ , $m_3/m_0 = 0.50$	External-internal supersonic compression, short-length diffuser. Low cowl projected area resulted from internal supersonic turning of flow.
CONFID. RM 857807A Lewis 10- by 10-foot supersonic wind tunnel		3	Flush slot and ram scoop at center-body shoulder	2.0 to 3.0	3.78	0°-15°	0	✓	✓	✓		At $M_0 = 3.0$ , $P_3/P_0 = 0.785$ ; at $M_0 = 2.0$ , $P_3/P_0 = 0.875$	At $M_0 = 3.0$ , $m_3/m_0 = 0.98$ ; at $M_0 = 2.0$ , $m_3/m_0 = 0.50$	External-internal supersonic compression, short-length diffuser. Low cowl projected area resulted from internal supersonic turning of flow.
CONFID. RM 857807A Lewis 10- by 10-foot supersonic wind tunnel		3	Flush slot and ram scoop at center-body shoulder	2.0 to 3.0	3.78	0°-15°	0	✓	✓	✓		At $M_0 = 3.0$ , $P_3/P_0 = 0.785$ ; at $M_0 = 2.0$ , $P_3/P_0 = 0.875$	At $M_0 = 3.0$ , $m_3/m_0 = 0.98$ ; at $M_0 = 2.0$ , $m_3/m_0 = 0.50$	External-internal supersonic compression, short-length diffuser. Low cowl projected area resulted from internal supersonic turning of flow.

#### Bibliography

These strips are provided for the convenience of the reader and can be removed from this report to compile a bibliography of NACA inlet reports. This page is being added only to inlet reports and is on a trial basis.

NASA Technical Library



3 1176 01435 8726

